



# Analysis of Cracking Causes in an Aluminium Alloy Bike Frame

S. Cicero<sup>a,\*</sup>, R. Lacalle<sup>a,b</sup>, R. Cicero<sup>a,b</sup>, D. Fernández<sup>a</sup>, D. Méndez<sup>a</sup>

<sup>a</sup>Universidad de Cantabria, ETS Ingenieros de Caminos, Canales y Puertos, Departamento de Ciencia e Ingeniería del Terreno y de los Materiales, Av/LosCastros s/n, 39005 Santander, Cantabria, Spain, <sup>b</sup>INESCO Ingenieros SL, Centro de Desarrollo Tecnológico de la Universidad de Cantabria (CDTUC), Fase A, Mod. 203, Av/Los Castros s/n, 39005 Santander, Cantabria, Spain

## ARTICLE INFO

### Article history:

Received 22 June 2010  
Received in revised form 9 July 2010  
Accepted 3 August 2010  
Published online 7 August 2010

### Keywords:

Bike Frame  
Stress Corrosion Cracking  
Solution Potential  
Overaging

## ABSTRACT

**The contents of this paper are only used as a demonstration of the GNU troff typesetting system.** Two cracks were detected in the bike frame of an amateur cyclist, before the final failure of the component and after using it for around 35,000 km. The cracks were located in the joint between the bottom bracket, the chain stays, the seat tube and the down tube.<sup>[1]</sup>

This paper analyses the causes of the cracking process and comprises, basically, chemical analysis for material identification, visual inspection of the frame, microstructural analysis, microhardness measurements, mechanical characterisation through Small Punch tests and SEM (plus EDX) analysis of the fracture surface.

The analysis concludes that both cracks were caused by corrosion and Stress Corrosion Cracking (SCC) processes that are justified by the differences in the solution potentials between the base material and equilibrium precipitates produced by an overaging treatment. The latter are more anodic and hence easily dissolved in a humid saline environment.<sup>[2]</sup>

© 2010 Elsevier Ltd. All rights reserved.

## 1. Introduction

After three years and around 35,000 km of service, two cracks were detected in the bike frame of an amateur cyclist. Both cracks were located in the joint of the bottom bracket with the chain stays, the seat tube and the down tube, and were detected before the in-service failure of the component. The bike was used in the north coast of Spain, and therefore, in a humid climate (average relative humidity around 80% over the year, precipitation of 1200/1300 mm/year, and 150/180 rainfall days per year) with a saline environment.



Fig 1. The bicycle being studied

Fig. 1 shows the bike frame and the location of the cracks, while Fig. 2 shows a detail of both cracks. It can be seen how the chain stays, the seat tube and the down tube are welded to the bottom bracket, generating a complex

geometry with numerous weld beads.

In Fig. 2, some indications of corrosion can be noticed in the interior of the bottom bracket and also in the vicinity of the cracks, in which the cyclist had performed a manual sanding, depriving these zones of the paint-layer. Fig. 3 presents the cracked section containing Crack 1,<sup>[3]</sup> which is the largest one. The extension of the crack and its approximate geometry can be observed here.

## 2. Chemical Analysis

Steel, aluminium alloys, titanium and carbon are the most used materials in bike frame fabrication. In the case being analysed, it was known that the material was an aluminium alloy (AA), but the specific alloy was not known. The use of AA provides light bike frames, with relatively simple fabrication processes, a wide variety of shapes and a significant stiffness provided by the high dimensions of the transversal sections used in the tubes.<sup>[4]</sup>

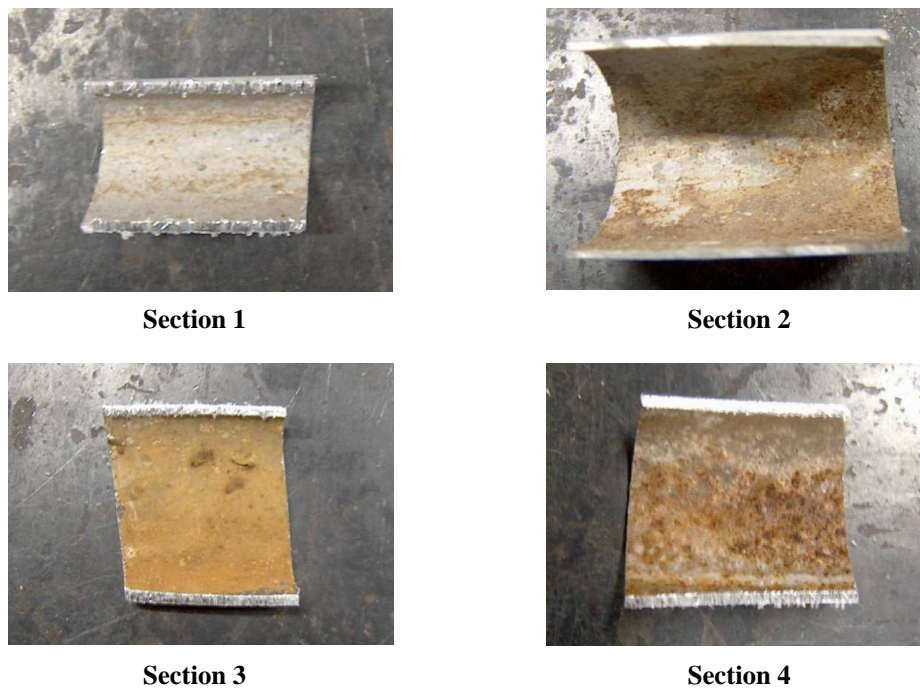


Fig 2. This is a section

### 3. Visual Inspection

As mentioned above, Fig. 2 shows indications of corrosion in the interior of the bottom bracket and also in the vicinity of the two detected cracks. In order to establish the extension of the corrosion processes occurring in the bike frame, several cuts were performed on it. Fig. 4 shows the inner part of the joint between the bottom bracket, the seat tube and the downtube, with a widespread, clear and extended corrosion process occurring in the entire internal surface.<sup>[5]</sup>

The rest of the cuts performed on the bike frame also revealed corrosion processes occurring all along the interior of the frame, in such a way that the closer to the bottom bracket, the more extended the corrosion process. Fig. 5 shows the corrosion level found in some of the locations. Likewise, Fig. 6 shows a hole found in the lower part of the bottom bracket. This hole provides an immediate access for the air, the water and the dirt to the interior of the tubes which, as shown in Fig. 4, were connected through additional internal holes. The hole shown in Fig. 6 explains the images shown in Fig. 5, given that the extension of the corrosion processes occurring on the different tubes depends on their corresponding proximity to the hole (that is, to the external environment).



**Fig. 3** Corrosion levels found in different tubes

### 4. EDX Results

Table 1 shows the EDX results for the three different types of precipitates, confirming that they are all equilibrium (b) pre-cipitates with high order compositions. It can be observed that the so-called large dark precipitates have very high contents of Si and Mg and lower contents of Al and Zn than AA 7005. The large bright precipitates have considerably high amounts of Si and Mn, and a surprisingly high content of iron. Finally, the small precipitates have significant amounts of Si and Mn. Therefore, the three different types of precipitates distinguished through the SEM images effectively correspond to three clearly different chemical compositions and their corresponding solution potentials. The table also gathers the chemical composition of the weld material, confirming that it is an AA of the 5xxx series (Mg alloyed), as suggested in Section 4.<sup>[6]</sup>

	Al	Zn	Mg	Mn	Si	Fe
Large dark precipitates	76.94	3.34	5.58	-	14.05	-
Large bright precipitates	71.57	2.87	0.66	4.66	4.76	15.48
Small precipitates	91.12	4.60	1.23	1.90	1.16	-
Weld material	96.10	-	3.90	-	-	-

**Table 1**

## References

1. F. Chang, Lih-Tyng Hwang, Chih-Feng Liu, Wei-Sheng Wang, Jeng-Nan Lee, Shun-Min Wang, and Kai-Yi Cho, "Design of a pipeline inspection robot with belt driven ridged cone shaped skate model," *IEEE* (2015).
2. M O Tatar and A Pop, "Development of an in pipe inspection minirobot," *IOP Conf. Series: Materials Science and Engineering* **147** (2016).
3. *Pipe Crawler - Ultrasonic Inspection Robots*, "<https://inspector-systems.com/pipe-crawler/ultrasonic-inspection-robots.html>" (2020).
4. Ankit Nayak and Sharad Pradhan, "Design of a New In-Pipe Inspection Robot," *ScienceDirect* (2014).
5. ULC Robotics, *Robot Cased Pipeline Inspection*, "<https://ulcrobotics.com/services/robotic-cased-pipeline-inspection/>".
6. Hui Li, Ruiqin Li, Jianwei Zhang, and Pengyu Zhang, "Development of Pipeline Inspection Robot for the Standard Oil Pipeline of China National Petroleum Corporation," *MDPI* (2020).